RECOGNITION OF AE SIGNALS FROM FATIGUE-CRACKED AND PATCH-REPAIRED ALUMINUM PANEL

Yongjoon Jang, Oh-Yang Kwon and Sung-Jin Kim

Department of Mechanical Engineering, Inha University
253 Yonghyun-dong, Inchon 402-751, Korea

Abstract

The fatigue crack growth behavior of a cracked and patch-repaired AA2024-T3 panel has been monitored by acoustic emission (AE). It was found that the overall crack growth rate was reduced and the crack propagation into the adjacent rivet hole was also retarded by introducing the patch repair. AE signals due to crack growth after the patch repair and those due to disbonding of the aluminum-patch interface were discriminated each other by using principal component analysis. The former showed higher center frequency and lower amplitude, whereas the latter showed longer rise time, lower frequency and higher amplitude. This type of signal recognition method can be effectively used for the prediction of fatigue crack growth behavior of the patch-repaired structures, with the aid of a nontraditional AE source location.

1. Intoduction

There has been increasing use of the composite-patch repair technique for damaged aircraft structures, where for example, a cracked aluminum panel can be reinforced by adhesively bonded composite laminates [1]. Composite-patch repair can homogeneously transfer load from the cracked panel to the patch and significantly reduce the possibility of corrosion and leakage by sealing up the interface with adhesive. In addition, composite-patch repair can increase the patch efficiency by adjusting the fiber orientation along the principal stress of the crack.

To maintain the reliability of composite-patch repaired structures, a real-time monitoring as well as the fatigue test has to be developed for the measurement and evaluation of crack growth. Various type of NDE methods including ultrasonic C-scan, infrared thermography, eddy current testing, radiography, guided wave ultrasonics were applied for the assessment of crack growth and the disbonding of aluminum-patch interface [2-5]. A study of the competitive relationship between the crack growth and the disbonding by discriminating the AE signals due to the re-growth of fatigue cracks from those due to the separation of repaired interface is yet to be developed for the practical use of such a technique in real-time.

2. Experimental procedures

The specimen used was AA2024-T3 Alclad panel of 350x 276x 1.6mm in size, with five simulated rivet holes of 3.2mm in diameter at 20mm interval along the horizontal centerline. The rivet hole was machined by electric discharge machining (EDM) and the surrounding scratches were completely removed by polishing to easily observe cracks by traveling microscope. Fatigue load was applied by a servo-hydraulic testing machine which enables a sinusoidal loading with the stress maximum of 102MPa in 5Hz and the stress ratio, R=0.2. Four AE sensors were attached on the surface of panel to form a rectangular array of 250x 160mm as shown in Fig. 1.

AE measurement was carried out by using a two-channel signal processing module (FTM4000; Digital Wave) with A/D board (CS225; Gage) in PC. AE sensors (B1025; Digital Wave) were broadband type with relatively flat response in 50kHz~2MHz frequency band. Detected AE signals were amplified by 40dB at the pre-amplifier and by 21dB additionally at the main-amplifier to be used for the AE source location and thereby the positions of crack initiation. Threshold was set at 0.1V in every experiment and trigger gain was amplified by 21dB considering noises originated from testing machine. AE signal waveforms were digitized at 5MHz sampling rate and stored as 2048 data. The initiation of cracks and their length at the surface of

panels were also measured by traveling microscope in 100x magnification whose image was enhanced by CCD camera. Crack images were recorded at the disk by using an image capture program (PowerVCR II). Fig. 2 shows a schematic diagram of experimental setup.

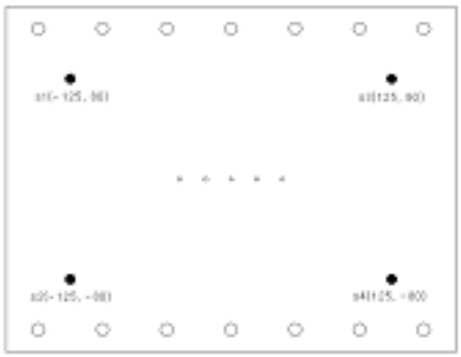

Figure 1: Geometry of the specimen with a rectangular array of AE sensors

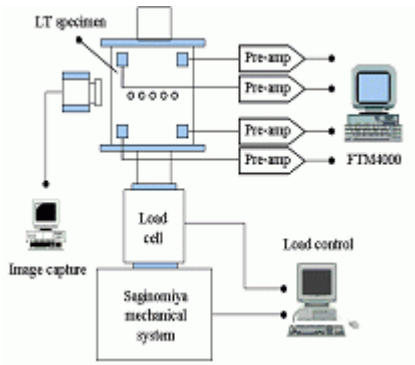

Figure 2: A schematic diagram of experimental setup

Two types of specimens (denoted as specimen #1 and specimen #2) were prepared for to investigate the effects of crack patching. Specimen #1 denotes a simply fatigue-tested aluminum panel with five rivet holes along the horizontal centerline as shown in Fig. 1, whereas specimen #2 denotes the aluminum panel fatigue-cracked firstly and then composite patch-repaired, respectively. Specimen #1 was tested under the fatigue load up to the point that the cracks initiated and grew to be connected through all the five rivet holes. Specimen #2 was prepared in two steps: the aluminum panel specimen was loaded under the fatigue testing condition stated above until the cracks initiated and grew independently less than 5mm, then was repaired with five-ply carbon/epoxy (UIN125B prepregs, SK Chemicals) laminate patch by using film adhesive (BMS5-101, Heatcon Composite Systems) followed by vacuum bag molding in autoclave. Appropriate surface treatment using sandpaper, acetone and MEK was applied at both the panel and the patch for perfect adhesion. Photographs of specimen #1 and specimen #2 are shown in Fig 3.

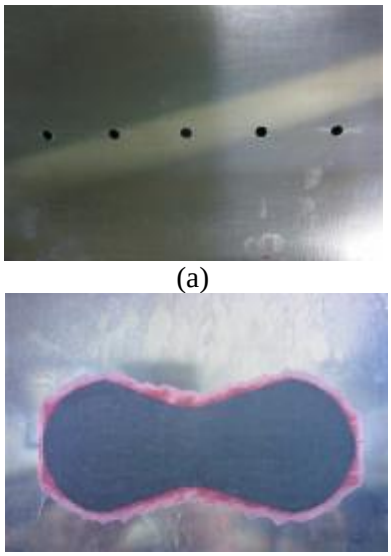

(a)

(b)

Figure 3: Photographs of the fatigue-cracked and the patch-repaired specimens; (a) before patching and (b) after patching

Specimen #2 whose data has been presented in this paper had four fatigue cracks at three rivet holes, the length of which were 5.04mm, 3.21mm, 2.1mm, 0.6mm. The ply thickness of laminate was 0.122mm so that the maximum thickness of the patch was 0.61mm. The bonded composite patch was designed to meet the design practices currently employed in the fields that give a repair-to-panel stiffness ratio of 1.10. The stiffness ratio is defined as $E_R t_R / E_P t_P$, where E and t are the Young's modulus and thickness, respectively, and the subscripts R and P denote the patch-repair and the aluminum panel. The patch was a unidirectional laminate with fiber orientation in loading direction and manufactured as a dog bone shape shown in Fig. 4.

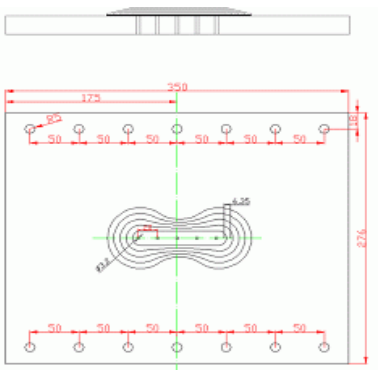

Figure 4: Geometry and dimension of the patched specimen

The patch was applied to one side of the panel covering all the fatigue cracks. The larger cover-ply

is common practice in composite- patch repair, protecting the underlying plies from damage as well as shielding the bondline from environmental attack. Fatigue testing condition for the specimen #2 was the same that was applied for the specimen #1.

Because there were five rivet holes in the panel specimens and the fatigue cracks can initiated at both sides of each hole, as many as ten cracks can be initiated. To denote a particular crack easily, each crack rivet hole was indicated by Roman numerals and each prospective crack position was indicated by Arabic numerals as shown in Fig 5 [6].

Figure 5: Numbers assigned to each hole and prospective crack position at both sides of each hole

3. RESULTS AND DISCUSSION

3.1 Effect of composite-patch repair

Fig. 6 shows the growth behavior of the cracks No. 10 in specimen #1 and specimen #2. The cracks had grown from the right side of hole V toward the patch edge. In specimen #1 the crack had grown to the length of 32.12mm during 45,000 fatigue cycles, whereas in specimen #2 it had grown to the length of 30.02mm during 137,000 cycles. It could be said that the fatigue life of specimen #2 was extended by approximately three times by introducing the composite-patch repair.

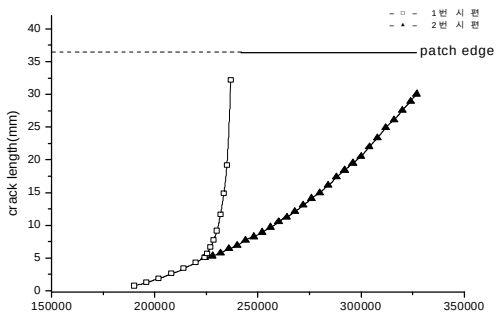

Figure 6: Growth behavior of the crack 10 in specimen #1 and specimen #2

Fig. 7 shows the growth behavior of cracks at adjacent holes being joined together during the fatigue testing of specimen #1 and specimen #2, respectively. It was actually the sequence of cracks joining at different holes from the Fig. 7(a) to the Fig. 7(d). In comparison to the result from specimen #1, the fatigue life was extended by 2.6 times for the first joining of (a), 3.6 times for the second joining of (b) in specimen #2.

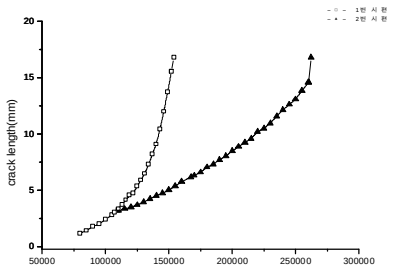

(a) Cracks No. 8 and No. 9 joined

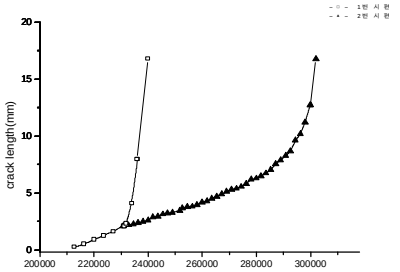

(b) Cracks No. 6 and No. 7 joined

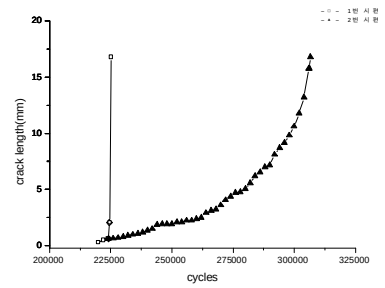

(c) Cracks No. 4 and No. 5 joined

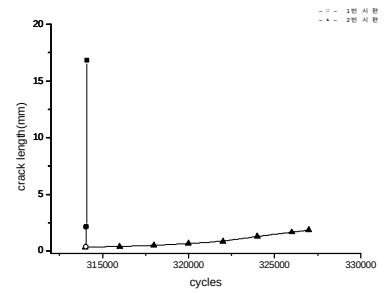

(d) Cracks No. 2 and No. 3 joined

Figure 7: Growth behavior of cracks being joined each other between adjacent holes

Once the cracks at any adjacent holes connected then the crack grew faster to be connected with the next adjacent hole in specimen #1, whereas in specimen #2 the crack growth was significantly retarded so that the fatigue cycles needed for any adjacent holes to be connected were much longer. With the third joining of (c), the patch-repaired

specimen #2 achieved an overall fatigue life of 90000 cycles after the cracked and patch-repaired condition, whereas the cracks in specimen #1 grew so fast that the holes were connected instantaneously. And even until the fatigue testing ended, namely until the last pair of holes were joined, fatigue life was significantly extended. The crack No. 10 grew only about 2mm up to the moment.

3.2 AE events with fatigue crack growth

More than 3000 AE signals were detected during the fatigue testing of specimen #1, but only 32 were detected with the specimen #2. Although cracks were still growing after the cracked panel was repaired by bonded composite patch, much fewer AE signals were detected from specimen #2. By speculating all the factors possibly affecting the result, it was assumed that the attenuation of signals due to the composite patch could significantly reduce the number of detectable signals. To confirm this, we examined waveforms generated by pencil-lead breaks at the positions both inside the patch and outside the patch. Peak amplitude from the unpatched shown in Fig. 9(a) was decreased by half in Fig. 9(b), which was from the patched. Crack signals are generally weaker than those from pencil lead breaks and easily disappeared before they reach the sensor. Only those AE signals due to the joining of adjacent holes could reach the sensor even after the severe attenuation since the joining might release much higher energy in such short time duration. This is thought to be the reason why the number of detectable AE signals was sharply decreased in patch-repaired specimens.

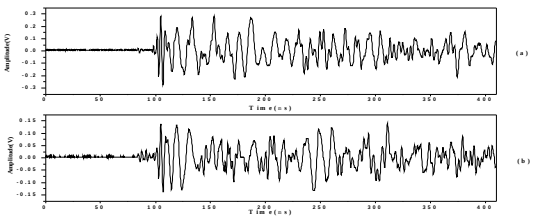

Figure 9: Effect of composite patch on the attenuation of simulated AE signals by pencil-lead breaks

To trace the origin of thirty-two (32) AE signals detected, the cumulative AE events and the length of fatigue cracks were compared in terms of fatigue cycles as shown in Fig. 10. Out of thirty-two signals, three (3) were found to be detected at around 62200 cycles, four (4) at around 78400 cycles, and one (1) at around 83800 cycles. These actually corresponded to the moment of joining of holes VI and V, III and VI, II and III, respectively. Therefore, eight out of thirty-two AE signals appeared to be originated from the joining of cracks, whereas the other twenty-four were thought to be resulted from the separation of the panel-patch interface in the vicinity of continuously growing cracks. It could be of interest that the crack growth in the aluminum panel and the separation of interface might be discriminated by the recognition of AE signals detected from the cracked and patch-repaired aluminum panel.

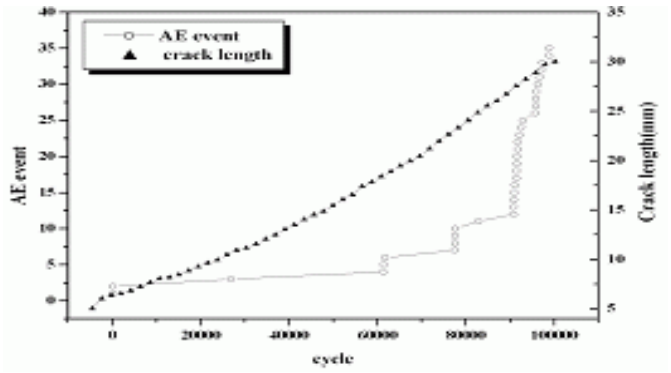

Figure 10: Cumulative AE events and the crack length vs. number of fatigue cycles

3.3 Source location of detected AE signals

Two-dimensional source location was carried out for the 32 detected AE signals to investigate the separation of interface between the pre-existing cracks and the patch, and the propagation of the separation boundary. Since the composite patch-repaired panel showed the anisotropy of different wave velocity along the directions in terms of fiber orientation, the nontraditional source location algorithm was applied with the wave velocities actually measured at the panel [7]. The patch was vertically symmetrical but horizontally unsymmetrical because there was a crack of 5.04mm at the position No. 10 but no crack at the position No. 1 when the panel was repaired and patch dimension was determined with the reference at the crack tips. In the nontraditional AE source location, the patch was taken as the region of interest (ROI) and the velocities at different directions at each 5°interval were measured from 10°up to 65°to completely include the ROI. The velocity changed from 2974.4 m/s, the highest at outside of the patch, to 2342.5 m/s, the lowest at the direction through the patch center.

With the velocities actually measured in this way, the accuracy of source location for the simulated signals by pencil-lead breaks was verified that the average error was 2.3mm, which is within the experimental error bound. When the conventional

source location with an isotropic velocity of 2980 m/s was performed for the 32 detected AE signals, the result appeared to be awfully bad as shown in Fig. 11(a). Except a few signals whose source point at or close to the center, the error of source location became very large. When the nontraditional AE source location with the anisotropic wave velocities was performed for the same data sets, all the source points were located within the patch and mostly located around the rivet holes.

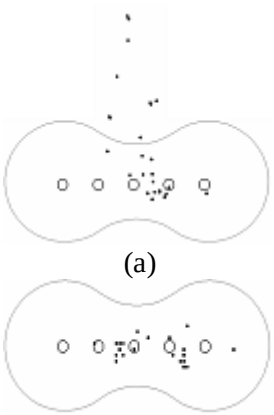

(a)

(b)

Figure 11: Results of source location in patch-repaired specimen: (a) conventional method and (b) nontraditional source location

3.4 Recognition of AE signals

AE signals acquired at various stages of with the same sensor before and after patch-repair are shown in Fig. 12. The number at the shoulder of each waveform indicates the fatigue cycles at which the signal was detected. Waveforms in Fig. 12(a) were acquired from specimen #1 during fatigue test, whereas those in Fig. 12(b) were detected during the fatigue test of specimen #2 that had been cracked and patch-repaired. The two groups of waveforms appeared not to be easily discriminated each other.

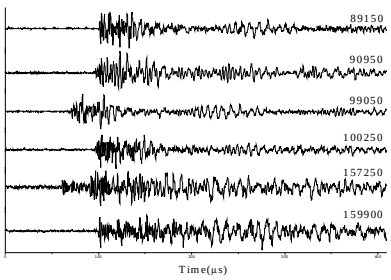

(a)

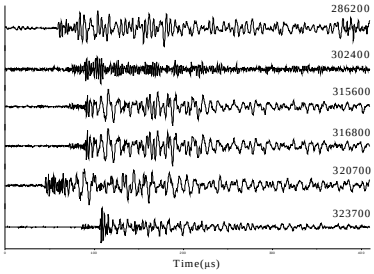

(b)

Figure 12: Series of waveforms detected at various stages; (a) before patching and (b) after patching

A few signals in Fig. 12(a) analyzed by FFT showed various frequency contents of 150-200kHz, 220-410kHz and so on. By using the coincidence appeared in Fig. 10, the signals generated during the crack growth showed a relatively wide range of frequency centered at 220-410kHz. On the other hand, the signals generated during the joining of adjacent holes after extensive growth of the cracks showed a relatively low frequency range of 150-200kHz. The amplitude was also reduced by 50% in Fig. 12(b).

To classify the group of signals due to fatigue crack growth and the group of signals due to the separation of the panel-patch interface, the principal component analysis (PCA) was introduced by utilizing the AE parameters. Data set for PCA consists of 42 AE signals including 10 from the fatigue testing of specimen #1 and 32 detected with the specimen #2. The parameters extracted from waveforms for PCA include FR(center frequency), PA(peak amplitude), RT(rise time), SR(peak amplitude/rise time ratio), EN(signal energy). Especially, FR was obtained from power spectral moment that the sum of power spectral density divided by the area below the power spectral density curve and RT was measured from the denoised waveforms by wavelet transform (bior3.9).

Since the result of correlation analysis between the five parameters showed PA had too high correlation coefficient of 0.66 and 0.86 with SR and EN, respectively, PA was deleted from the parameters for PCA. The result of PCA for the 42 signals is shown in Table 1. The first and the second principal components cover more than 85% of the total data variation.

Table 1 Eigenvalues of principal components

Principal component	Eigenvalue	Percentage proportion
1	1.9266	48.17
2	1.4915	37.29
3	0.38345	9.58
4	0.19845	4.96

The feature-feature plot for the signals from patch-repaired Al panel by using the first and the second principal components is shown in Fig. 13. Signals detected during the fatigue testing of specimen #1 and during the joining of adjacent rivet holes in specimen #2 were classified as in the same group with negative value of the second principal component and widely spread value of the first principal component. On the other hand, those appeared to be generated by the separation of the panel-patch interface were confined within the narrow range of both the first and the second principal components. The former group of signals showed shorter rise time (RT), higher center frequency (FR) and relatively lower energy (EN), whereas the latter group of signals showed longer RT, lower FR, and relatively higher energy.

Actually many AE signals except those due to the joining of cracks at adjacent holes became undetectable due to severe attenuation. At the final stage of fatigue testing of specimen #2, however, after the joining of holes Ⅳ and Ⅴ, holes Ⅲ and Ⅳ, holes Ⅱ and Ⅲ, relatively large number of 24 signals were detected. With the comparison of the result of AE source location (Fig. 11) and that of PCA (Fig. 13), crack signals were mostly concentrated around the holes Ⅳ and Ⅴ, which was joined at the earliest. Disbonding signals were concentrated around the cracks No. 4 and No. 5 at the final stage. This implies the sequence of fatigue damage development; with the crack growth adjacent holes joined together and finally the bonded interface between the panel and the patch would be separated. With the result of precise AE source location, the classification of crack signals and disbanding signals by PCA can provide the recognition of AE signal.

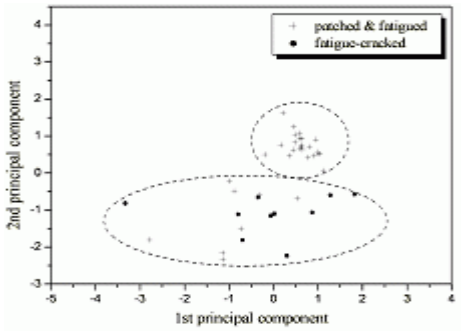

Figure 13: Feature-feature plot for the patch-repaired Al panel by the first two principal components

4. CONCLUSIONS

1. Fatigue life of a cracked and composite patch-repaired aluminum panel was increased at least 2.5 times, which could be affected by the patch efficiency.
2. Despite the continuous growth of fatigue cracks, detectable AE hits were reduced due to the high attenuation of signals by the composite patch present on the way from source to sensor.
3. The source points of AE signals were located around the rivet holes by using the nontraditional source location algorithm for anisotropic plate.
4. Signals due to crack growth after patch-repair and those due to disbonding of the panel-patch interface were successfully discriminated each other by using principal component analysis. The former showed higher center frequency and lower amplitude, whereas the latter showed longer rise time, lower frequency and higher amplitude.

REFERENCES

[1] A.A. Baker, Advances in the Bonded Composite Repair of Metallic Aircraft Structure, Elsevier, Oxford, UK, pp. 1-18, 2002
[2] J.J. Schubbe and S. Mall, Proc. 39th AIAA SDM Conf., pp. 2434-2443, 1998
[3] C. Soutis, D-M. Duan, and P. Goutas, Composite Structures, Vol. 45, pp. 289-301, 1999
[4] J.L. Rose, K. Rajana, and J.N. Barshinger, Rev. of Prog. in QNDE, Vol. 15, pp. 1291-1298, 1996
[5] N. Rastogi, S.R. Soni, and J.J. Denney, Proc. 39th AIAA SDM Conf., pp. 1578-1588, 1998
[6] J.-C. Kim, Oh-Yang Kwon and S.-J. Kim, J. of the KSNT, Vol. 23, No. 3, pp. 246-253, 2003
[7] Oh-Yang Kwon, Progress in Acoustic Emission XII, JSNDI, Tokyo, Japan, pp. 1-6, 2004
[8] Oh-Yang Kwon and S.-H. Lee, NDT&E International, Vol. 32, pp. 153-160, 1999